# NASA DebriSat – Verification of Material Characterization Processes by Utilization of Machine Learning Algorithms

**Bogachan Ondes(1), Kutsal Dogan (2), Rafael Carrasquilla(1), and Norman Fitz-Coy (1)**

(1) The University of Florida Department of Mechanical and Aerospace Engineering, 939 Center Dr, Gainesville, FL, USA - bogachan.ondes@ufl.edu
(2) The University of Florida, Warrington College of Business, 1384 Union Road, Bryan Hall 100, Gainesville, FL, USA – Kutsal.Dogan@warrington.ufl.edu

**Abstract**

The DebriSat project was created by NASA, DoD, The Aerospace Corporation, and the University of Florida to provide characteristic data to improve orbital debris modeling capabilities. A test article known as DebriSat, a mock up satellite, was designed and fabricated to be representative of a modern-day low Earth orbiting satellite and subjected to a hypervelocity impact test (HVI) at the Arnold Engineering Development Complex (AEDC) in Tennessee. The foam supporting panels and fragments of DebriSat test article were collected and transported to the University of Florida for extraction and characterization. Fragments are individually assessed for material, shape, mass, and size (cross-sectional area, volume, and characteristic length) and recorded in Debris Categorization System (DCS)[1]. At later stages of fragment characterization, a bias related to material selection was detected. This manuscript demonstrates the method for mitigating this bias and provides a ML based solution for future material characterization work.

## 1 Introduction

The fragment material assessment at DebriSat project is mostly qualitative since there is a requirement for not damaging fragments during extraction. Primary methods for assessment were to measure the mass and volume of the fragment by operators' efforts using the DebriSat mass and imaging sub-systems. After a brief survey, it was seen that the majority of the CRFP fragments were primarily needle-like or flat plates in shape. Since needle-like and flat plate fragments have small heights ($Z_{DIM}$), 2D imaging systems were developed and utilized to collect top and side view images of these thin fragments to calculate the volume by multiplying top views cross-sectional area with $Z_{DIM}$. Since these fragments were mostly uniform in the side view, volumes were calculated with high accuracy. Although this method was very high speed and efficient for thin flat fragments, it lacked the capability to output the true volume calculations for more complex geometries, such as metal nuggets and entangled wires.

While the true volumes were known to be not accurate, operators would use their before impact knowledge about the DebriSat test article and try their best to characterize metals. However, during HVI testing a layer of char was formed on the exterior of most fragments, which led to some confusions in determining metals by their appearance. Thus, the most reliable differentiating factor was density for characterizing metals. However, one of the biggest issues with density was the volume calculation that resulted in density ranges for each metal group. The operators use these given ranges for different metals; however, there are samples that are significantly close to bounds of the tolerated densities, which makes it challenging for operators to decide.

### 1.1 Dimensional Analysis with 2D Imager

The 2D imager consists of a single point shoot camera, a mirror placed on a 45° wedge, an up pointing led backlight, a glass plaque for fragment placement, a calibration ring, and an upstanding white screen for side view background. A 2D imager is shown below in Fig. 1.

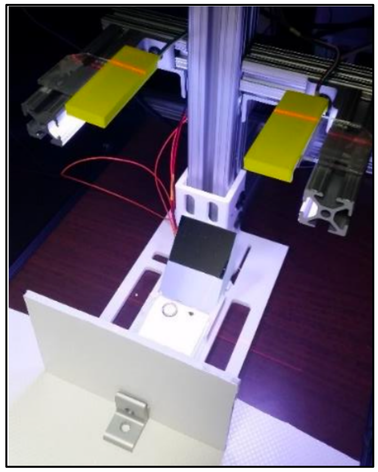

*Fig. 1. 2D Imager [1]*

A 2D imager captures two views per object, a top view, and a side view. Dimensional analysis is completed by an automated MATLAB software. As, shown in Fig. 2 the $X_{DIM}$ is measured by finding the largest distance between two points on the plan view cross-sectional area and $Y_{DIM}$ is measured by finding the largest distance between two points that is orthogonal to the $X_{DIM}$ line. The $Z_{DIM}$ (height) is measured by finding largest distance between two points on the side view [3].

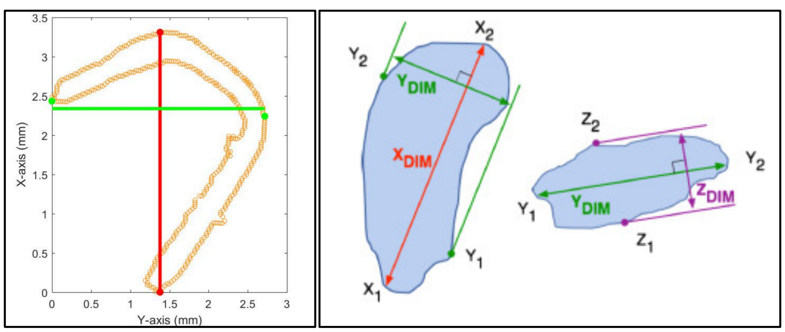


*Fig. 2. 2D Imager Dimensional Analysis [4]*

The 2D imager also measures the plan view cross-sectional area by counting pixels of the top view image. This area is referred as pixel area ($PA$). Fragment volume is calculated by multiplying plan view cross-sectional area (pixel area) by fragment height ($Z_{DIM}$).

$$Volume = Pixel\ Area\ (PA) * Z_{DIM} \tag{1-1}$$

In 3D geometrical sense, this volume calculation method creates a prism by extruding the plan view by the amount of height. This method would estimate the volumes of flat plates and prismatic objects.

However, if a fragment is not perfectly prismatic this method always overestimates the volume as shown in Fig. 3.

A 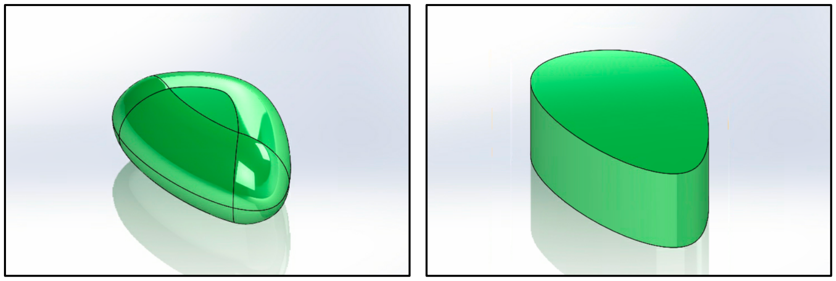 B

*Fig. 3. A) A Hypothetical Fragment and B) Volume Representation which would Result from 2D Imager Volume Calculation*

Moreover, this volume overestimation cannot account for cavities and may significantly overestimate the height depending on the sideview. As Fig. 4 illustrates, a bent plate is showing larger volume due to the sideview geometry where for this fragment a height measurement that is significantly greater than the fragment's thickness is used.

A 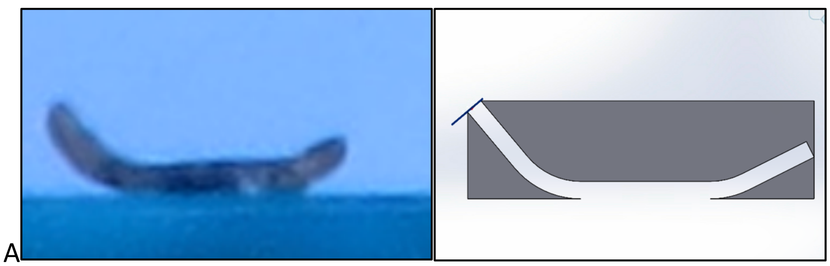 B

*Fig. 4. DS133981 Side View and Overestimated Volume Visualized (Right).*

## 2 Bias Analysis

At later stages of DebriSat project, rising counts in verified titanium fragments have caught attention. After a search in the DCS and debris repository, two of the original titanium pieces were found. As Fig. 5 and Fig. 6 shows, except one mount is missing a small portion, titanium mounts have stayed intact after the HVI.

A 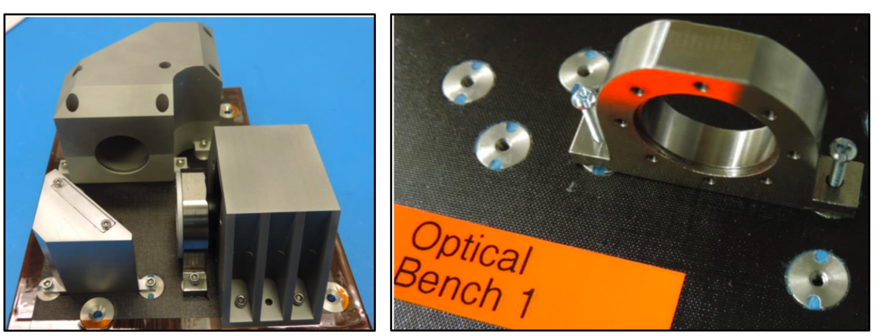 B


*Fig. 5. Titanium Camera Mounts Before HVI (Moises, 2018) [2]*


*Fig. 6. Titanium Camera Mounts After HVI*

These findings have motivated an investigation on verified 2D titanium fragments. The investigation of 79 titanium labeled verified fragments has revealed that no fragment was titanium and labels were selected due to biased fragment densities. The volume overestimation has appeared to have caused underestimation of the density.

Since density is an important measure for selecting labels for metal fragments, true volume estimation is crucial for determining the material type. A first approach of re-estimating volumes was inspired by DS117391 (Fig. 7 and Fig. 8), a sphere-shaped fragment.

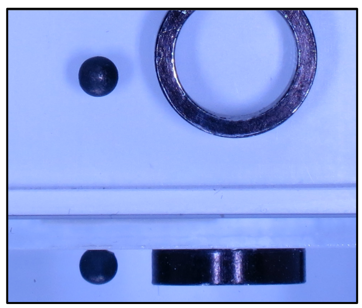

*Fig. 7. DS117391*

MEASUREMENTS

| | | | | | | | | |
|---|---|---|---|---|---|---|---|---|
| Mass: | 0.130681 | g | Temp: | 24.60 | °C | RH%: | 35.60 | % |
| $X_{DIM}$: | 3.194 | mm | $Y_{DIM}$: | 3.173 | mm | $Z_{DIM}$: | 2.979 | mm |
| $L_C$: | 3.116 | mm | Volume: | 23.225 | $mm^3$ | Density: | 0.005627 | $g/mm^3$ |
| ACSA: | 11.630 | $mm^2$ | AMR: | 88.998 | $mm^2/g$ | | | |

*Fig. 8. DS117391 Measurement Data*

The fragment is showing $0.0056\ \mathrm{g/mm^3}$ for its density and was labeled titanium. However, recalculation of geometry as a sphere shows the fragment label should be stainless steel.

$$X_{DIM} \approx Y_{DIM} \approx 3.18\ mm \ \Rightarrow\ \emptyset \approx 3.18\ mm$$
$$True\ Volume_{DS117391} = \frac{4\pi}{3} * \left(\frac{3.18\ mm}{2}\right)^3 \cong 16.84\ mm^3 \qquad (2\text{-}1)$$
$$\rho_{DS117391} = \frac{0.013g}{16.84\ mm^3} \cong 0.0077\frac{g}{mm^3}$$

DS117391 was mislabelled due to the density bias. It is a unique fragment for having a spherical geometry. However, fragments seldom appear in common 3D shapes. As shown in Fig. 9, the same type of stainless-steel spring washers yield three different metal labels (stainless-steel, titanium and aluminum) when density is considered as the sole decision making criterion.

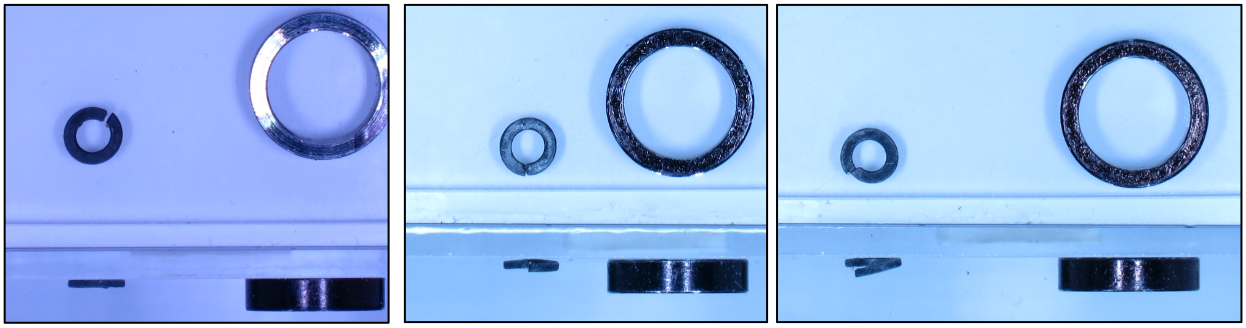

*Fig. 9. From Left to Right; DS172465, DS113636, DS143034*

*Table 1. Fragment Densities*

| | DS172465 | DS113636 | DS143034 |
|---|---|---|---|
| Density ($g/mm^3$) | 0.0061 | 0.0044 | 0.0029 |

While these fragments are visually identifiable to be fasteners, most metal fragments are broken and have lost its original shape during the impact. When a fragment loses its original shape, visual identification becomes challenging. Therefore, it is critical to improve the volume estimations.

## 3 Dynamic Volume Algorithm

The study on various fragments has revealed that the volume overestimation varies. The operators at DebriSat project may be biased towards making decisions on material type, however, they are able to tell whether a fragment consist of one or more material. Thus, if the dataset is constrained to have single metal, there would be three classes (titanium, aluminum, stainless steel). (Fig. 10)

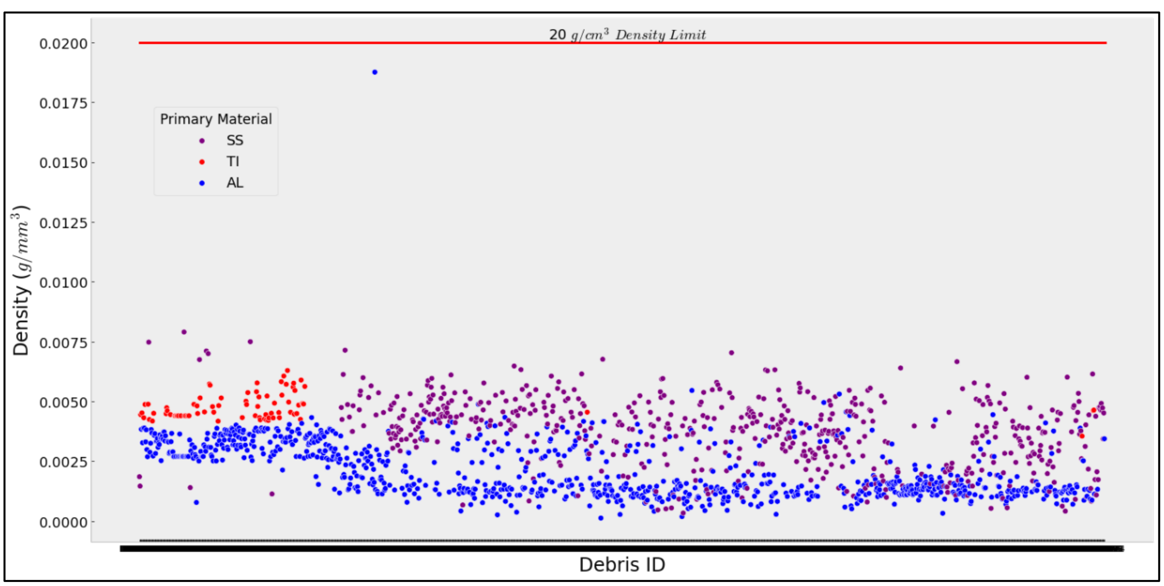


*Fig. 10. Database Density Chart of 2D Verified Metal Dataset*

Given these materials have ideal densities, an algorithm was developed to estimate the volume based on fragment densities. The 2D imager overestimates the volume, yet, it has accurate $X_{DIM}$, $Y_{DIM}$ and $Z_{DIM}$ measurements. Considering how $X_{DIM}$, $Y_{DIM}$ and $Z_{DIM}$ are measured, an assumption is made that an ellipsoid which fits to these dimensions could encapsulate the fragments true volume. The resulting chart from density calculations with ellipsoidal volumes can be seen in Fig. 11.

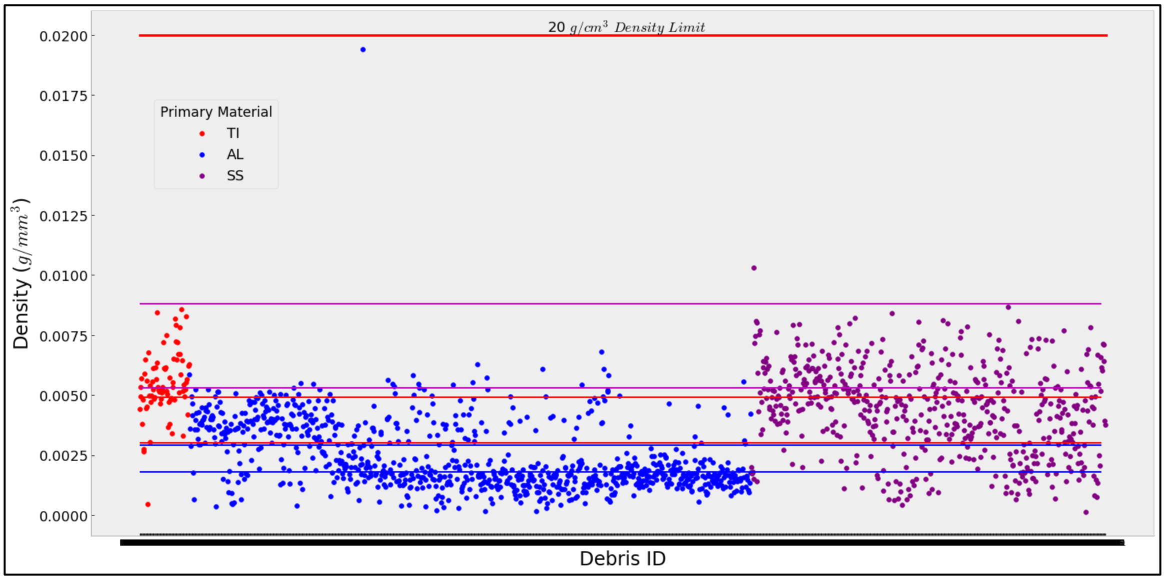


*Fig. 11. Fragment Densities Calculated by Ellipsoidal Volumes*

Apart from one fragment, all fragments are under the stainless-steel upper density limit. The ellipsoid encapsulation assumption is valid. However, the true volume would occupy some percentage of the ellipsoid. Based on materials in the set, fragments should either belong to aluminum density region or stainless-steel density region. An algorithm called "Dynamic Volume" (DVOL) was developed to place fragments into these categories by setting their volumes to 50% ellipsoidal and incrementally inflate the volume until the fragment came to a reasonable area on the density chart.

Wire volumes are not well estimated with ellipsoids. Plan view of bent wires would overestimate the $Y_{DIM}$ and would make 50% ellipsoid volume to be much less than the true volume. Thus, another subroutine was established for wire-like fragments within DVOL. The subroutine would estimate the length of the wire from plan view and use that length to get the diameter by dividing pixel area to the length.

$$\emptyset_{Wire} \cong \frac{CSA}{Length_{Wire}}$$

$$Volume_{Wire} = \pi * \left(\frac{\emptyset_{Wire}}{2}\right)^2 * Length_{Wire} \tag{3-1}$$

$$\rho_{Wire} = \frac{mass_{Wire}}{Volume_{Wire}}$$

The estimation was not always accurate, yet it still took stainless steel fragments from aluminum region. Wire length estimation needs optimization and is still in progress, therefore wires are assigned at a place holder density value (0.01 $\mathrm{g/mm^3}$). The resulting chart of DVOL based densities (DYD – dynamic density) is shown in Fig. 12.

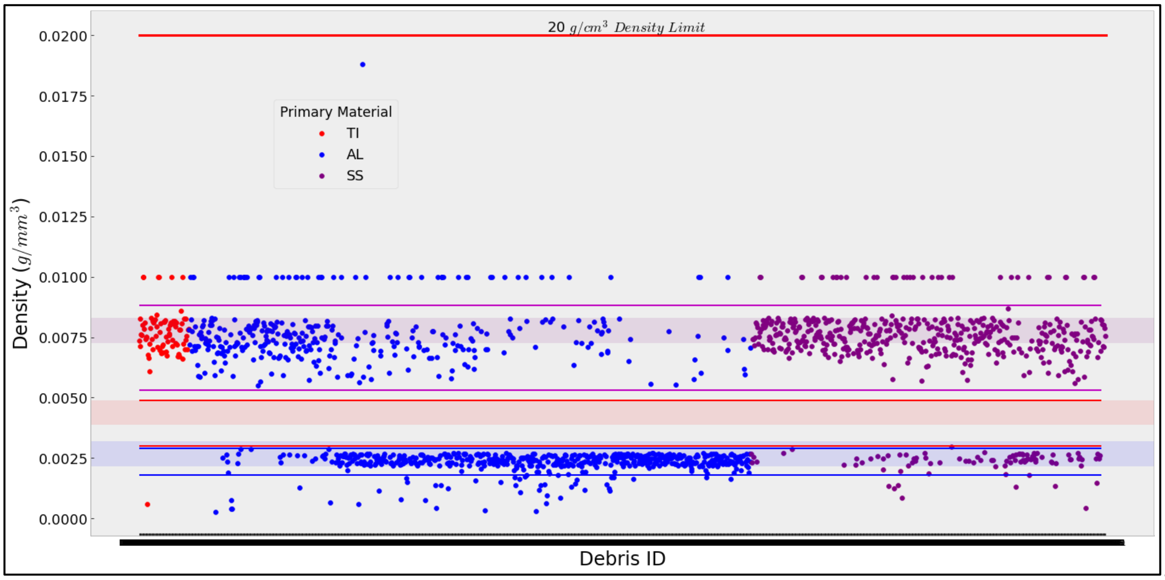


*Fig. 12. DVOL Density Chart*

The DVOL algorithm has brought many stainless-steel fragments from the aluminium region to the stainless steel region and brought all except one titanium labelled fragments to the stainless steel region. Considering titanium parts are mostly found intact and the separation between aluminum and stainless-steel is visible, these labels are more consistent. As Fig. 13 shows, fragments returned to their original densities while the labels are modified according to DVOL results.

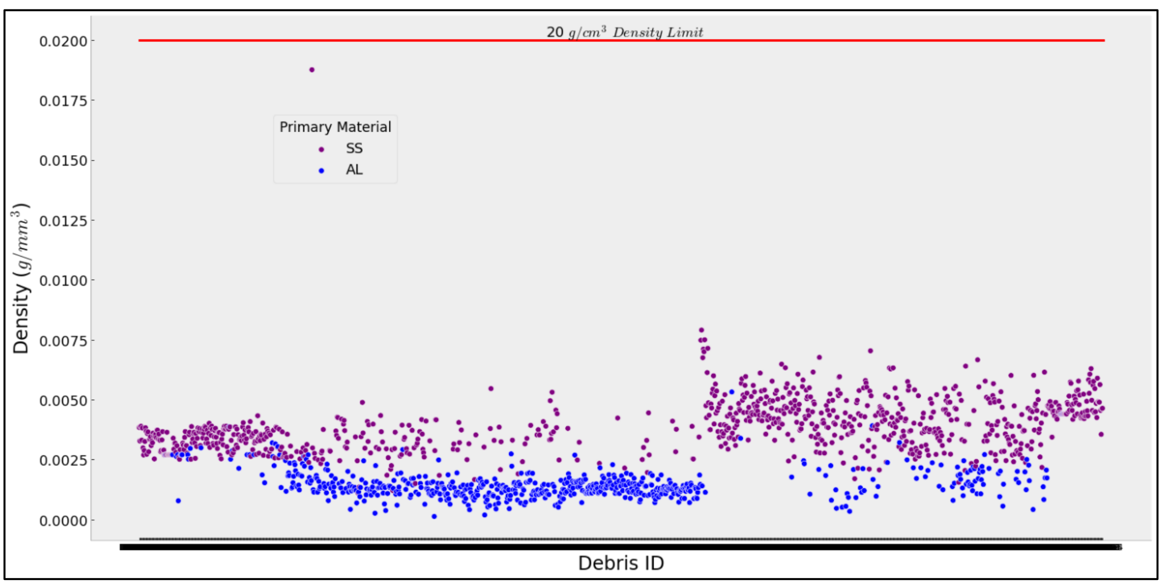


*Fig. 13. Material Labels after DVOL Application*

There are metal fragments in the DCS that are yet to be labeled and verified. It is desired that the bias will not be present for the verification of remaining fragments, i.e., operators shall not mislabel. One of the ways to avoid bias is utilization of machine learning (ML). A supervised machine learning (ML) model requires true labels, as DVOL mitigated the bias for labels, this pre-verification set can be subject to a machine learning model for material prediction. By the knowledge that there are no titanium fragments in the dataset, logistic regression (a binary classifier) algorithm was found to be the best algorithm for material prediction [5].

## 4 Machine Learning for Material Labeling

The dataset was engineered for ML algorithm; the string data columns were encoded, and all data was scaled by standard scalar. The DYD and DVOL columns were dropped to avoid biasing the predictions. The DYD resulted labels were set as the target. The data was divided into two sets: 50% for training set and 50% for test set. The training was cross validated 5 times to get the best fit. The test results can be viewed at Table 2. The results are promising since an accuracy over 90% is considered a good model [5]. Thus, the model is ready to be applied on the "METAL" subset, which are shown as black data points in Fig. 14. The model was examined with a confusion matrix that provided a detailed breakdown of its classification performance, showing the number of true positives, true negatives, false positives, and false negatives for each class in the classification task.

Table 2: Good Model – Test Set Results

| Labels | Precision | Recall | F1-Score | Support |
|---|---|---|---|---|
| AL | 0.94 | 0.96 | 0.95 | 316 |
| SS | 0.97 | 0.98 | 0.96 | 449 |
| Accuracy Scores | | | 0.95 | 764 |
| Macro Average | 0.95 | 0.96 | 0.95 | 764 |
| Weighted Average | 0.95 | 0.95 | 0.95 | 764 |

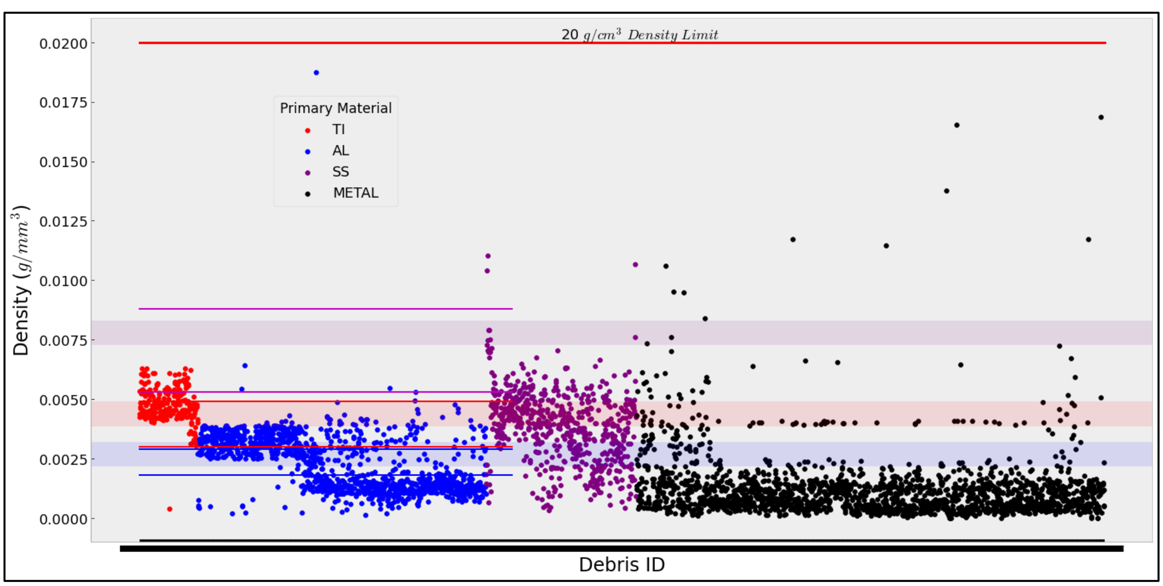


*Fig. 14. Overall 2D Metal Fragments Dataset*

### 4.1 ML Results

The confusion matrix is a measure of performance for ML predictions, it shows whether prediction labels are matching with the true labels [5]. The numbers on the diagonal cells indicate how many fragments were predicted correctly. The ML models cannot predict labels that are not in the training dataset and since the metal dataset has fragments in the very low-density region it has difficulty properly identifying them. For example, these low-density fragments may be multi-material fragments and have metal visual features, such as MLI which were not accounted for in the initial DCS entry. Since the trained model only have aluminium and stainless steel as prediction labels, it is likely to see more aluminium predictions due to low density feature.

As it is seen at Fig 15, the confusion matrix shows 200 stainless steel predictions out of metal labelled fragments. The DYD values were not included into the training dataset to avoid bias, therefore the indexes of the predictions were compared to the table where DVOL values were present. This comparison has revealed that 166 out of 200 predictions had densities in the stainless steel region with their DYD values. Predictions caught 10 fragments with noisy measurement data, these are the fragments that have very high densities. These fragments should be reimaged before the verification stage; therefore, they shall not be included to the accuracy calculations. Thus, it can be concluded that the ML model was successful to predict stainless steel fragments with base accuracy of 87% (166/190).

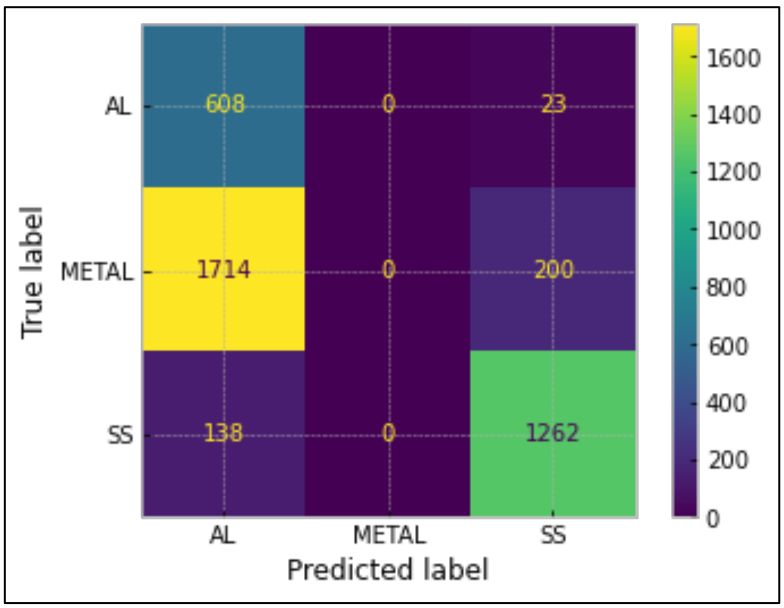


*Fig 15. Model Predictions out of Metal Dataset*

## 5 Conclusion and Future Work

This manuscript has shown the method to mitigate volume calculation errors caused by 2D imager. It has been shown that the volume is always overestimated if the fragment is not perfectly prismatic. This volume overestimation has caused density underestimation, which led to the bias for labeling fragments. A DVOL algorithm was developed to re-estimate true volumes of the fragment for resolving density bias and labels were modified with respect to DVOL results. A ML model was developed for making predictions from unlabeled metal fragments dataset. The ML model results have been compared to DVOL results and it was shown that the model have successfully detected stainless steel fragments.

The future work will include training the operators on findings from this study and improvements in the ML model. Considering metal dataset might have glass and MLI, models' ability to predict aluminum will need improvement. Logistic regression model can be extended to whole dataset, where all material labels may be introduced to the training dataset. Other ML algorithms, such as Decision Tree or K-Nearest Neighbor, may also be utilized for validating the results of logistic regression.

## 6 References


1. J. Kleespies, " Design, Development, and Implementation of the DebriSat Debris Categorization System " Master's Thesis, Dept. of Electrical and Computer Engineering, Univ. of Florida, Gainesville, 2018.
2. M. A. Rivero, "DEBRISAT: Fabrication of a Representative LEO Satellite." Master's Thesis, Dept. of Mechanical and Aerospace Engineering, University of Florida, 2018.
3. Ralen Toledo, Bungo Shiotani, Norman Fitz-Coy "Imaging Systems Utilized in the DebriSat Fragment Size Characterization Process", First International Orbital Debris Conference. Sugar Land, TX. 2019.
4. Samantha Allen, Norman Fitz-Coy, "DebriSat fragment characterization: Quality assurance", Journal of Space Safety Engineering, Volume 7, Issue 3, 2020, Pages 235-241, ISSN 2468-8967, https://doi.org/10.1016/j.jsse.2020.08.001.
5. Scikit-learn: Machine Learning in Python, Pedregosa et al., JMLR 12, pp. 2825-2830, 2011.